

SYNTHESIS AND STUDIES ROOM TEMPERATURE CONDUCTIVITY, DIELECTRIC ANALYSIS OF LaF₃ NANOCRYSTALS

Sidheshwar G. Gaurkhede

Department of Physics, Bhavan's College of ASC,
Andheri (W) Mumbai-400058. India

s.gaurkhede@gmail.com

PACS 61.05.cp, 77.22.d

Lanthanum fluoride (LaF₃) was synthesized using LaCl₃ and NH₄F as starting materials in de-ionized water as solvent via a microwave-assisted technique. The structure of LaF₃ nanocrystals, analyzed by XRD and TEM, was found to be hexagonal with an average crystalline particle size of 20 nm (JCPDS standard card (32-0483) of pure hexagonal LaF₃ crystals). The resistivity and conductivity at room temperature for LaF₃ was verified and found to depend on the applied DC field. At an applied voltage of 20 V/cm – 30 V/cm, the resistivity and conductivity changes rapidly due to the liberation of extra fluoride (F⁻) ions, whereas the conductivity of LaF₃ nanocrystals depends upon temperature. The variation of dielectric constant (ϵ') and dielectric loss (ϵ'') with applied frequency shows normal dielectric behavior, attributable to the space charge formation. The observed peak in the plot of tangent loss ($\tan \delta$) vs. $\log F$ around 2.6 KHz can be attributed to interface charge relaxation at the grain boundaries.

Keywords: Microwave radiation, Hexagonal shape, X-ray diffraction, Dielectric materials.

Received: 24 November 2014

Revised: 28 November 2014

1. Introduction

Lanthanum fluoride based chemical sensors have potential to be widely used in applications such as the detection of fluorine, oxygen, and carbon monoxide, due to its high chemical stability and ionic conductivity [1]. The ionic conducting nature of the rare earth fluorides (solid electrolyte) is exploited as sensor materials to construct various electrochemical sensors like gas sensors, biosensors, and ion selective electrodes [2]. Lanthanum fluoride is an excellent F⁻ ionic conductor among other rare earth fluorides [3]. Miura et al. reported the use of lanthanum fluoride film in biosensor and room-temperature oxygen sensor based on its high F⁻ ion-conducting properties. The working principle of LaF₃ based biosensors and oxygen sensors is explained as the movement of F⁻ ion conduction [4, 5]. Fedorov P. P. [6] et al. review the major aspects of inorganic chemistry of nanofluorides, methods of synthesis, including nanochemical effects, preparation of 1D, 2D, and 3D nanostructures, surface modification of the nanoparticles, fluoride nanocomposites and applications of nanofluorides. The orthorhombic β -YF₃ structure and ionic conductivity of rare earth fluorides and of tysonite-structured were investigated by Trnovcova et al. [7, 8]. At room temperature, the ionic conductivity of single crystals of tysonite-type solid solutions La_{1-x}Ba_xF_{3-x} has been studied and no exchange occurs between different types of anion sites in the tysonite structure [9, 10]. Very recently, Kumar et al. [11, 12] attempted to synthesize lanthanum fluoride nanoparticles by the simple method of direct precipitation in aqueous solution. The impedance, modulus and dielectric spectra analysis

of the prepared LaF₃ nanoparticles has been studied using AC impedance spectroscopy. The ionic conductivity of LaF₃ nanoparticles were reported to be significantly increased by an order of magnitude, from 10⁻⁶ S cm⁻¹ to 10⁻⁵ S cm⁻¹. The modulus and dielectric spectra analysis confirmed the non-Debye type behavior in the material. The synthesized LaF₃ nanoparticles exhibited hexagonal shape and red luminescence. In the present case, LaF₃ nanoparticles have been synthesized using a conventional microwave radiation technique for first time.

2. Experimental

2.1. Synthesis of Nanocrystals

Synthesis of LaF₃ nanocrystals follows an aqueous route and uses a microwave heating at low power range. The method is simple and cost effective. Water soluble LaCl₃ and NH₄F are mixed to obtain a solution in 1:3 molar ratio [13]. To a 10 ml homogenous solution of 0.64 mol LaCl₃ in de-ionized water in a 100 ml beaker was added a 10 ml solution of 0.192 mol NH₄F in a drop-wise manner via a funnel fitted with a stopper to control the rate of dripping, and placed the whole set up inside a conventional microwave set at low power range (in on-off mode set at 30 sec) for around 30 min. The low power range setting largely helped us avoid spill-over of the solution. A white ultrafine crystalline precipitate identified as doped LaF₃ nanocrystals appeared almost instantly, having settled to the bottom of the beaker. The white precipitate was then washed several times with de-ionized water and absolute methanol, and was then dried in a microwave oven for approximately 15 minutes. The dried sample was then stored in sealed ampoules for further characterization and analysis.

2.2. Characterization

Powder X-ray diffraction (XRD) measurements have been performed using a PANALYTICAL X'PERT PROMPD diffractometer model using CuK α radiation $\lambda = 1.5405$ Å. U with a scanning rate of 2 ° per min in the 2 θ range from 0 ° to 80 °. Transmission electron microscope (TEM) analysis was performed at different magnification by PHILIPS (CM 200) 0.24 nm resolution, operating at 200 kV. The dielectric constants of the sample have been measured using sophisticated Hioki 3532 LCR Meter. The capacitance and dissipation factor of the parallel plate capacitor formed by sample as a dielectric medium was measured.

3. Result and Discussion

The XRD pattern obtained from the LaF₃ nanocrystals shown in Fig. 1. The results of the XRD are in good agreement with the hexagonal LaF₃ structure as described in the reports LaF₃ (JCPDS card No. 32-0483) [14]. The average crystallite size was estimated from the Scherrer equation, $D = 0.90\lambda/\beta \cos \theta$, where D is the average crystallite size, λ is the X-ray wavelength (0.15405 nm), θ and β being the diffraction angle and full width at half maximum of an observed peak, respectively. The strongest peak (111) at $\theta = 27.84$ ° for LaF₃ samples were used to calculate the average crystallite size (D) of the nanoparticles [15]. The average crystallite sizes of LaF₃ nanoparticles are 20 nm, which is in agreement with the TEM and SEM results. The XRD pattern of the LaF₃ nanoparticles is nearly similar to that of LaF₃: Ce³⁺, Tb³⁺ [16]. No XRD signals are observed for impurity phases.

Figure 2 shows the transmission electron microscopy (TEM) image of LaF₃ nanocrystals. Hexagonal, assorted and spherical shape nanocrystals with average particle size of about 21 nm were found. Fig. 3 shows the selected area electron diffraction (SAED) pattern. Three strong diffraction rings, corresponding to the (002), (111) and (300) reflections were observed, which

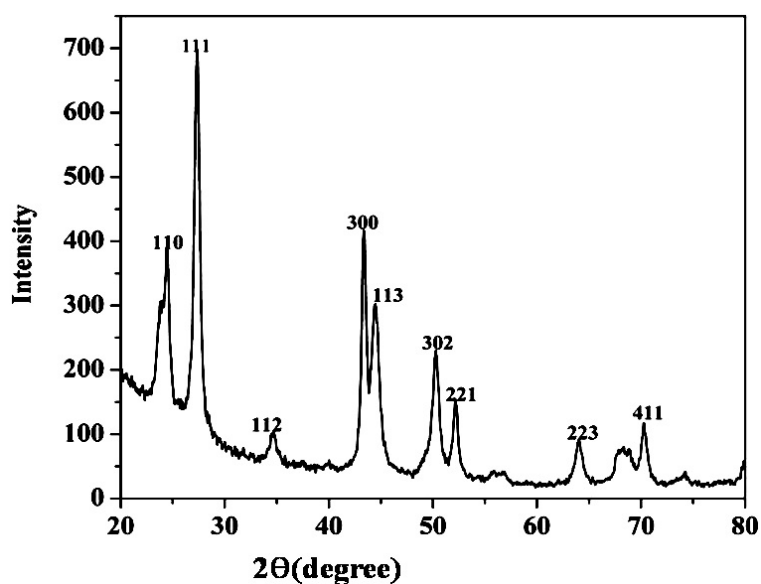


FIG. 1. X-ray diffraction pattern of LaF_3 nanocrystals

is in close agreement with the hexagonal LaF_3 structure [17]. This shows that the original structure of LaF_3 may be retained even after modification.

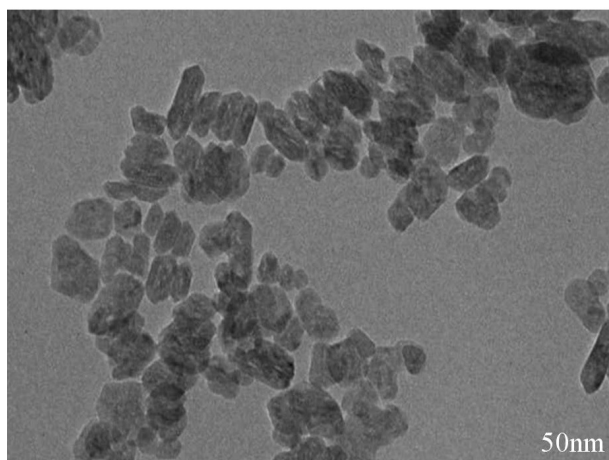


FIG. 2. TEM image of LaF_3 nanocrystals

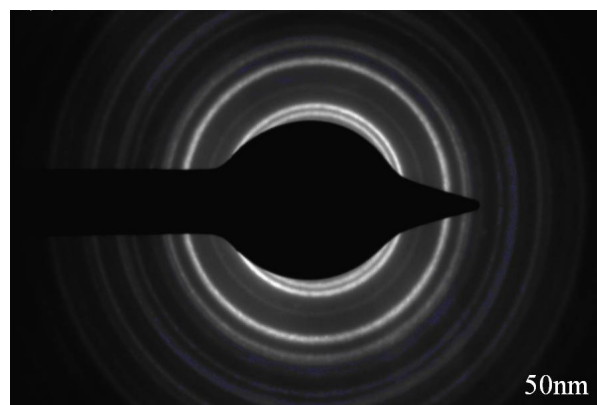


FIG. 3. Selected area electron diffraction (SAED) pattern image of LaF_3 nanocrystals

I – V characteristic of LaF_3 nanocrystals synthesis in deionized water and methanol is shown in Fig. 4. Conductivity / resistivity depended on the applied DC field. The ionic conductivity was calculated using the relation $\sigma_{dc} = t/RA$. Where, R is the measured resistance, t be the thickness of the pellet (cm) and A is the area of the pellet (cm^2) in contact with the electrode. The conductivity at room temperature of the sample prepared in deionized water was found to be $2.7 \times 10^{-6} \text{ S cm}^{-1}$, in agreement with previously-reported work. The conductivity was found to be $8.0 \times 10^{-6} \text{ S cm}^{-1}$, nearly four times higher in methanol than in de-ionized water samples at room temperature. The current was found to increase with the applied field [11]. The conductivity and resistivity were thus found to depend on the applied field. At an applied voltage of about 20 V/cm – 30 V/cm the conductivity / resistivity was found to change rapidly due to liberation of extra fluoride (F^-) ions [12].

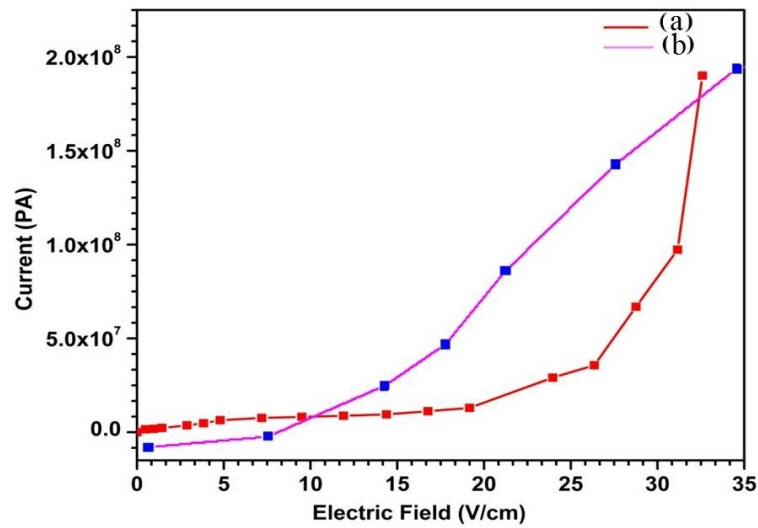


FIG. 4. Current vs. Voltage graph of LaF_3 nanocrystals prepared in (a) de-ionized water (b) methanol

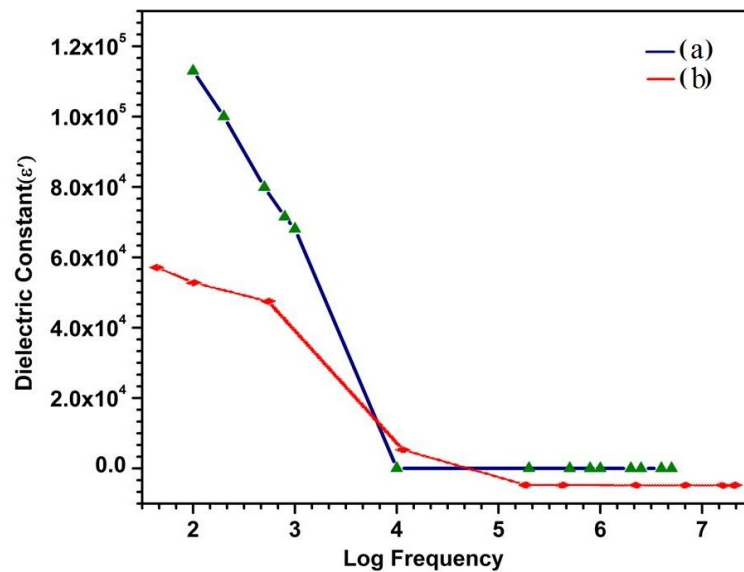


FIG. 5. Variation of dielectric constant with $\log F$ for LaF_3 nanocrystals prepared in (a) de-ionized water (b) methanol

The variations of dielectric constant in log frequency at room temperature for LaF_3 nanocrystals prepared in de-ionized water and methanol have been studied. Fig. 5 and Fig. 6 shows the plot of dielectric constant ϵ' as a function of log frequency and the plot of dielectric loss ϵ'' as a function of log frequency for LaF_3 nanocrystals. Both dielectric constant and dielectric loss exhibited similar variation with frequency, both being inversely proportional to frequency. This is normal dielectric behavior, that both ϵ' and ϵ'' decrease with increasing frequency. The dielectric constant was found to fall more rapidly as compared to dielectric loss with applied frequency.

A plot of $\tan \delta$ against $\log F$ is shown in Fig. 7. The relaxation peaks were found to lie near 2.6 KHz. From the figure, the peak in the low frequency region indicates the contribution of the real dielectric constant of the material due to the polarization [18].

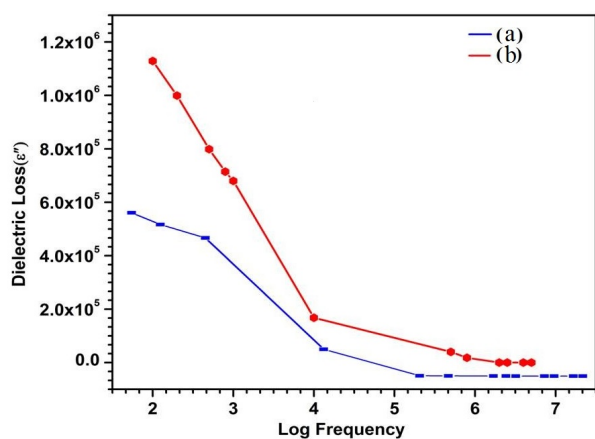


FIG. 6. Variation of dielectric loss with $\log F$ for LaF_3 nanocrystals prepared in (a) methanol (b) de-ionized water

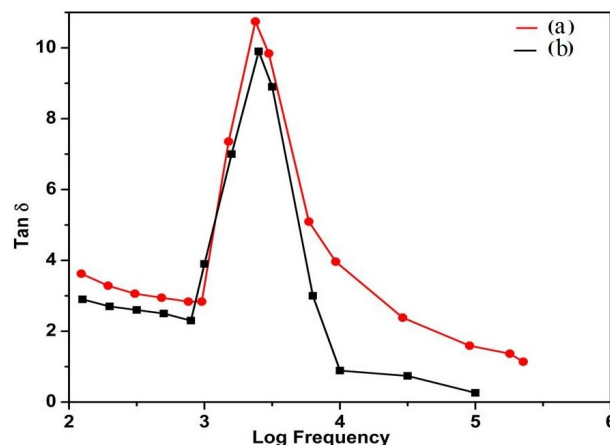


FIG. 7. $\log F$ versus $\text{Tan } \delta$ for LaF_3 nanocrystals prepared in (a) de-ionized water (b) methanol

4. Conclusions

LaF_3 nanocrystals were successfully synthesized using LaCl_3 & NH_4F in deionized water. Elongated & assorted size hexagonal geometry of LaF_3 nanocrystals were observed. XRD and TEM studies indicated that the average particle size was 20 nm. The conductivity at room temperature for LaF_3 sample prepared in deionized water was found to be in close agreement with reported values. This is the first report of conductivity varying with the applied field. With an applied frequency, the variation of ϵ' and ϵ'' shows normal dielectric behavior, attributable to space charge formation. A very sharp peak in the plot of tangent loss ($\tan \delta$) vs. $\log F$ has been noted around 2.6 KHz which can be attributed to interface change relaxation at grain boundaries.

References

- [1] Yamazoe N., Miura N. Environmental gas sensing. *Sensors Actuators*, **20** (2), P. 95–102 (1994).
- [2] Fergus J.W. The Application of Solid Fluoride Electrolytes in Chemical Sensors. *Sensors Actuators*, **42** (2), P. 119–130 (1997).
- [3] Schoonman J., Oversluizen G., Wapenaar K.E.D. Solid electrolyte properties of LaF_3 . *Solid State Ionics*, **1** (3), P. 211–221 (1980).
- [4] Miura N., Hisamoto J., Yamazoe N., Kuwata S. LaF_3 sputtered film sensor for detecting oxygen at room temperature. *Appl. Surf. Sci.*, **33/34**, P. 1253–1259 (1988).
- [5] Miura N., Hisamoto J., et al. Solid-state oxygen sensor using sputtered LaF_3 film. *Sensors Actuators*, **16** (4), P. 301–310 (1989).
- [6] Fedorov P.P., Luginina A.A., Kuznetsov S.V., Osiko V.V. Nanofluorides. *J. Fluorine Chem.*, **132** (12), P. 1012–1039 (2011).
- [7] Trnovcova V., Garashina L.S., et al. Structural aspects of fast ionic conductivity of rare earth fluorides. *Solid State Ionics*, **157** (1–4), P. 195–201 (2003).
- [8] Trnovcova V., Fedorov P.P., Furara I. Fluoride Solid Electrolytes. *Russian Journal of Electrochemistry*, **45** (6), P. 630–639 (2009).
- [9] Duvel A., Bednarcik J., Sepelk V., Heitjans P. Mechano-synthesis of the Fast Fluoride Ion Conductor $\text{Ba}_{1-x}\text{La}_x\text{F}_{2+x}$ From the Fluorite to the Tysonite Structure. *J. Phys. Chem. C*, **118** (13), P. 7117–7129 (2014).
- [10] Roos A., Pol F.C.M. van de, Keim R., Schoonman J. Ionic Conductivity in Tysonite-type Solid Solutions $\text{La}_{1-x}\text{Ba}_x\text{F}_{3-x}$. *Solid State Ionics*, **13**, P. 191–203 (1984).

- [11] Selvasekarapandiana S., Vijayakumara M., et al. Ion conduction studies on LaF₃ thin film by impedance spectroscopy. *Physica B*, **337** (5), P. 52–57 (2003).
- [12] Kumar D.A., Selvasekarapandian S., Nithya H., Hema M. Synthesis, micro-structural, and electrical analysis on lanthanum fluoride. *Ionics*, **18** (5), P. 461–471 (2012).
- [13] Meng J., Zhang M., Liu Y. Hydrothermal preparation and luminescence of LaF₃:Eu³⁺ nanoparticles. *Spect. Acta A*, **66** (1), P. 81–85 (2007).
- [14] Daihua T., Liu X., Zhen Z. Oleic acid (OA)-modified LaF₃ : Er, Yb nanocrystals and their polymer hybrid materials for potential optical-amplification applications. *J. Mater. Chem.*, **17** (1), P. 1597–1601 (2007).
- [15] Daqin C., Yuansheng W., En Ma, Yunlong Y. Influence of Yb³⁺ content on microstructure and fluorescence of oxyfluoride glass ceramics containing LaF₃ nano-crystals. *Mater. Chem. Phys.*, **101** (9), P. 464–469 (2007).
- [16] Pi D., Wang F., et al. Polyol-mediated synthesis of water-soluble LaF₃:Yb,Er upconversion fluorescent nanocrystals. *Materials Letters*, **61** (6), P. 1337–1340 (2007).
- [17] Yuanfang L., Wei C., et al. X-ray Luminescence of LaF₃:Tb and LaF₃:Ce, Tb Water Soluble Nanoparticles. *J. Appl. Phys.*, **103** (6), P. 1–7 (2008).
- [18] Kumar D.A., Selvasekarapandian S., et al. Dielectric, modulus and impedance analysis of LaF₃ nanoparticles. *Physica B: Condensed Matter*, **405** (17), P. 3803–3807 (2010).